Snapshots of modern mathematics
from Oberwolfach

№ 7/2020

Shape space – a paradigm for character animation in computer graphics

Behrend Heeren • Martin Rumpf

Nowadays 3D computer animation is increasingly realistic as the models used for the characters become more and more complex. These models are typically represented by meshes of hundreds of thousands or even millions of triangles. The mathematical notion of a *shape space* allows us to effectively model, manipulate, and animate such meshes. Once an appropriate notion of *dissimilarity measure* between different triangular meshes is defined, various useful tools in character modeling and animation turn out to coincide with basic geometric operations derived from this definition.

1 Introduction

Seeing artificial character animations created through advanced techniques from computer graphics is by now an everyday experience. The artists in television and film studios, for example, create virtual characters of dramatically increasing complexity, and design animations whose features are almost indistinguishable from natural figures, shapes, and motions. The development of flexible and effective tools to support artists in these tasks is linked to the mathematics

of *shape spaces*. Simply speaking, a shape space is a set with a mathematical structure whose elements are geometric shapes. In computer graphics, the most basic representation format for these geometric shapes are triangle meshes, as shown in Figure 1.

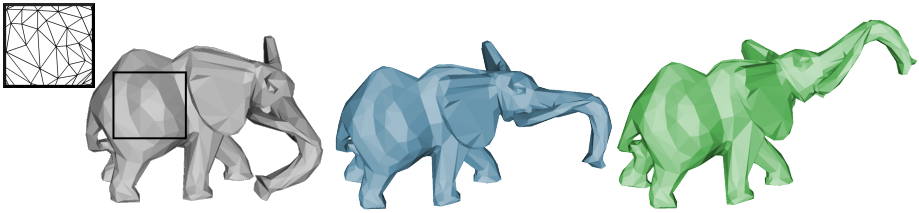

Figure 1: A typical geometric model used in computer graphics in three different poses (all represented as triangular meshes as indicated by the enlargement).

The term *mathematical structure* refers to the notion of a "local" dissimilarity measure that quantifies small variations of a particular shape. Once a "small variation" can be realized and quantified, one can derive more complex mathematical operations from it. For example, one can accumulate a sequence of small variations to describe a larger motion of the shape. The accumulated local dissimilarity measure then provides a notion of a "length" of this motion path. Finally, one can also define a "global" distance measure between two arbitrary shapes by means of the shortest path length between them.

Figure 2: Accumulating small variations to generate a complex motion or large deformation. Here, the color encodes a measure of local variations (red means high). The accumulated local dissimilarity measure between consecutive shapes then leads to a global distance measure between the two boundary shapes (leftmost and rightmost hand).

To this end the starting point for the mathematical processing of geometric models is the following question: can we define a meaningful (local) dissimilarity measure between "nearby" shapes in a shape space? For example, in what way does it make sense to say that the grey shape in Figure 1 is more similar to the blue one than to the green one?

A rich theory of the mathematics of shape spaces has been developed starting with the work of David George Kendall (1918–2007) in the 1980s [12]. In the last twenty years, several mathematicians have advanced the understanding of spaces of shapes. Here, the notion of shape includes planar curves [16, 15, 1], smooth surfaces [14, 2], images [17, 19], or triangle meshes [13].

In this snapshot, we report on a shape space calculus which is based on the notion of a "discrete path". Following a discrete path can be thought of as transitioning between finitely many shapes like between frames of a movie; for example, the sequence of hands in Figure 2 is a discrete path with nine shapes. Furthermore, one needs a suitable quantity called the *(discrete) path energy* defined on these discrete paths. This energy is defined to be the accumulated dissimilarity of consecutive shapes along the discrete path and shall serve as a *path selection criterion*, which means we will navigate between shapes by choosing discrete paths that minimize the path energy.

To enter the mathematical theory of shape spaces we proceed as follows. At first, guided by geometric intuition, we will study shortest discrete paths on the surface of the Earth and motivate the notion of a discrete path energy. Then, we will discuss the space of shapes described through potentially very large triangular meshes with a physically meaningful definition of a dissimilarity measure.[1]

2 Shortest paths and a discrete path energy on the surface of the Earth

Let us consider one of the simplest curved surfaces: a two-dimensional sphere in three dimensional space $\mathbb{R}^3$. The surface of the Earth, for example, can be modelled reasonably as a sphere, depending on the application. Aircraft undertaking long distance flights travel along shortest paths to save fuel. These shortest paths are segments of great circles – the circles obtained as the intersection of the surface of the Earth with two-dimensional planes passing through the center of the Earth.

Now we consider a discrete path $(x_0, x_1, \ldots, x_n)$ of points on the sphere, and assume that we travel between consecutive points along great circles, see Figure 3. Then we call the total distance traveled from the starting point x_0 to the end point x_n the *length* of the path and write

$$L := \sum_{i=1}^{n} d_i,$$

[1] We have published a series of papers on this topic which are the foundation and primary source of contents as well as graphical results presented in this snapshot, see [10, 8, 9].

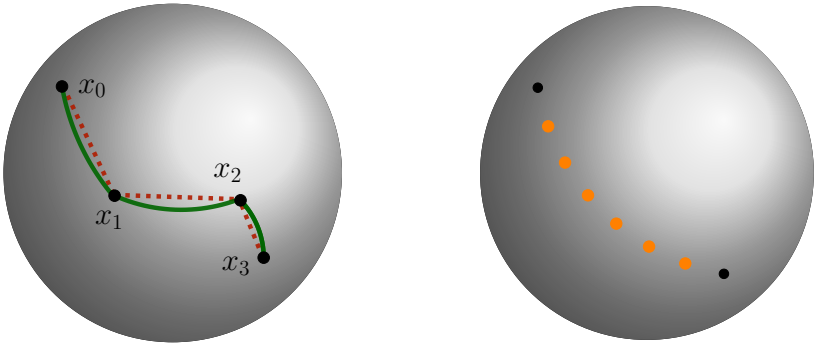

Figure 3: Left: A sketch of a *discrete* path on the sphere (points of the path are connected with segments of great circles in **green**. The dotted lines in **red** show the corresponding straight line segments through the interior of the ball). Right: A shortest discrete path with six intermediate points (**orange**) connecting two given end points (black).

where $d_i = \operatorname{dist}(x_{i-1}, x_i)$ is the distance along the segment on a great circle from x_{i-1} to x_i. We can also define the corresponding *path energy* to be

$$E := n \sum_{i=1}^{n} d_i^2.$$

It can be shown[2] that we always have the inequality

$$L \leq \sqrt{E}.$$

From this we deduce that a discrete path between fixed end points x_0 and x_n is of minimal path energy E if it already is of minimal length L with $L = \sqrt{E}$. In particular, all points x_i must lie on a common great circle. Note that the length does *not* change if we move the intermediate points $x_1, \ldots, x_{n-1}$ along that great circle (while keeping the order fixed), thus the terms d_i may change while the sum L stays the same. On the other hand we have[3] $L = \sqrt{E}$, that is, the energy is minimal, if and only if $d_i = L/n$, that is, if the points are distributed with equal distances along the discrete path. In summary, this means a discrete path having minimal path energy consists of equally distributed

[2] This inequality can be proven using the *Cauchy–Schwarz inequality* $\langle X, Y \rangle \leq \|X\| \cdot \|Y\|$ between the inner product $\langle X, Y \rangle$ of of two vectors X and Y in $\mathbb{R}^n$ and the product of their lengths, taking $X = (1, 1, \ldots, 1)$ and $Y = (d_1, d_2, \ldots, d_n)$.

[3] In the Cauchy–Schwarz inequality, equality holds if and only if X and Y differ by a constant factor.

points, whereas this might not be the case for a discrete path having minimal length. To this end, minimizing the path energy turns out to be a more suitable objective since in applications one is interested in uniformly distributed points (which correspond to a smooth transition).

However, from a computational point of view the evaluation of the squared length $\mathrm{dist}^2(x, \tilde{x})$ of the great circle segment between points x and $\tilde{x}$ is very costly.[4] Fortunately, we can use a suitable approximation $\mathcal{W}$ of dist^2, such as the squared Euclidean norm $\mathcal{W}(x, \tilde{x}) = \|x - \tilde{x}\|^2$ of the vector that joins x and $\tilde{x}$ in space (compare the dotted red lines in Figure 3). In fact, the closer two points get, the better the Euclidean distance approximates the length of the segment on the corresponding great circle. Replacing dist^2 by $\mathcal{W}$ in the definition of the path energy E, we arrive at a new discrete path energy

$$\mathbf{E} = n \sum_{i=1}^{n} \mathcal{W}(x_{i-1}, x_i)\,.$$

In the case of two-dimensional surfaces embedded in three-dimensional space, the definition of the approximation $\mathcal{W}$ is quite intuitive. However, in general shape spaces (where single points x_i represent geometric shapes), the definition of $\mathcal{W}$ is a challenging task. This $\mathcal{W}$ is exactly what we call a dissimilarity measure.[5]

3 From the surface of the Earth to the space of shapes

Let us now move from points on the two-dimensional sphere in $\mathbb{R}^3$ to shapes viewed as points in a very high-dimensional space of shapes. We think of a shape as a triangular mesh, which is a widespread and computationally very practical notion in computer graphics applications. Each shape is then described by a large vector X gathering the three-dimensional coordinate vectors $x_j \in \mathbb{R}^3$ of all N vertices (that is, $j = 1, \ldots, N$) of the mesh:

$$X = (x_1, \ldots, x_N)\,.$$

Given a mesh with N vertices, it follows that X is a vector in $\mathbb{R}^{3N}$. We assume here that any other shape $\tilde{X}$ in the particular shape space under consideration can be obtained via a deformation of the shape X, where the positions of the vertices can be changed, but not the *connectivity*, that is, the way they are connected to each other.

---

[4] For each evaluation of $\mathrm{dist}^2(x, \tilde{x})$ one has to solve an optimization problem by first finding the shortest path connecting x and $\tilde{x}$ and then returning its squared length.

[5] Mathematically, a dissimilarity measure $\mathcal{W}$ is an approximation to a squared distance measure but with fewer properties. For example, $\mathcal{W}$ does not have to be symmetric.

If we want to quantify the dissimilarity between two triangular meshes represented by vectors $X = (x_1, \dots, x_N)$ and $\tilde{X} = (\tilde{x}_1, \dots, \tilde{x}_N)$, respectively, then the squared Euclidean norm $\sum_{j=1}^{N} \|x_j - \tilde{x}_j\|^2$, which measures the sum of the squared distances of all pairs of vertices, is not a suitable dissimilarity measure. For example, if $\tilde{X}$ is obtained from X by a rigid rotation in space, the Euclidean distance between X and $\tilde{X}$ can be very large, although the actual shape of the mesh has not changed. In particular, the notion of "shape" should be independent of rotations and translations.

In our setup, we want $\mathcal{W}(X, \tilde{X})$ to quantify the "physical distortion" caused by a change of the vertex positions. In fact, we envision two different types of distortion: the first caused by stretching or compressing of the triangular facets (called *membrane distortion*) and the second induced by "bending". Stretching and compressing of a triangular mesh can be quantified in terms of the change of edge lengths, while bending (for example of two adjacent triangles) can be measured via the change of the dihedral angle between the triangle facets at the common edge. With this in mind, we split $\mathcal{W}$ into two components

$$\mathcal{W} = \mathcal{W}_{\text{mem}} + \mathcal{W}_{\text{bend}}$$

and define each of them as a sum over all edges of the underlying mesh to quantify a distinct local dissimilarity of the shapes X and $\tilde{X}$.

More precisely, let $\mathcal{E}$ be the set of edges of the triangulation, $l_e[X]$ denote the length of the edge e of the triangular mesh X, $\theta_e[X]$ be the dihedral angle between the two triangular facets meeting at the edge e, and $a_e[X]$ be the area of one third of these two triangles (marked in dark orange, see Figure 4 below).

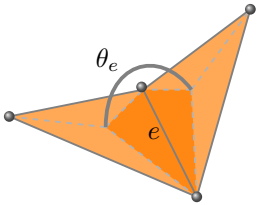

Figure 4: Illustration of the area a_e (in dark orange) and the dihedral angle θ_e for an edge e used in the definitions of $\mathcal{W}_{\text{mem}}$ and $\mathcal{W}_{\text{bend}}$, respectively. The triangles are subdivided at their respective barycenters.

Furthermore, having a length $l_e[X]$ and an area $a_e[X]$ associated with an edge e, we can formally associate a "height" to every edge via $h_e[X] =$

$a_e[X]/l_e[X]$ and set

$$\mathcal{W}_{\text{mem}}(X, \tilde{X}) = \sum_{e \in \mathcal{E}} a_e[X] \left(\frac{l_e[X] - l_e[\tilde{X}]}{l_e[X]} \right)^2 ,$$

$$\mathcal{W}_{\text{bend}}(X, \tilde{X}) = \sum_{e \in \mathcal{E}} a_e[X] \left(\frac{\theta_e[X] - \theta_e[\tilde{X}]}{h_e[X]} \right)^2 .$$

Both terms can be interpreted as a numerical integration over the mesh X, where $a_e[X]$ is the integration weight (or discrete area element) and the squared term measures a relative change of the objective quantities, that is, change of edge length and dihedral angle, respectively. In fact, $\mathcal{W}_{\text{mem}}$ quantifies the stretching or compression of each triangle when changing the vertex positions from X to $\tilde{X}$, while $\mathcal{W}_{\text{bend}}$ measures the bending of the triangle mesh, which gets larger as the angle between two adjacent triangles changes.[6] See Figure 5 for an illustrative example.

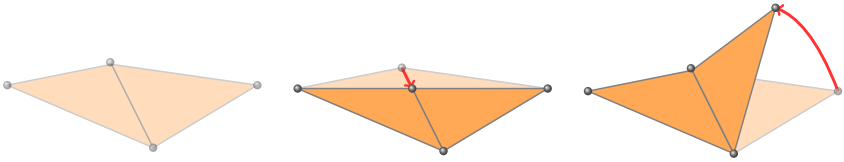

Figure 5: Two different kind of deformations of a flat reference stencil given by two adjacent triangles in the plane (left, with transparency): pure membrane distortion by compressing the common edge in the plane (middle; $\mathcal{W}_{\text{mem}} \approx 1/9$, $\mathcal{W}_{\text{bend}} = 0$) vs. pure bending distortion by a rotation about the common edge (right; $\mathcal{W}_{\text{mem}} = 0$, $\mathcal{W}_{\text{bend}} \approx \pi^2/9$).

An example of a shortest discrete path of deformations of a triangular mesh, which minimizes the discrete path energy $\mathbf{E}$ and is based on the definition of $\mathcal{W}$ that we have just given, has already been presented in Figure 2. In detail, we have computed a morphing/blending between two given end shapes X_A and X_B by computing a shortest discrete path $(X_0, \ldots, X_n)$ having $(n+1)$ shapes with $X_0 = X_A$ and $X_n = X_B$ being fixed.

[6] In fact, the bending term is an approximation of a quantity called the "Willmore energy", which measures differences in mean curvature. For a formal derivation and a convergence analysis we refer to [3, 7].

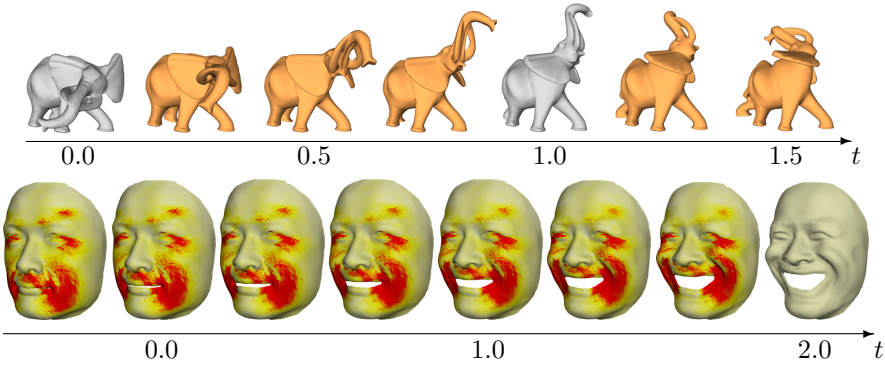

Figure 6: "Morphing" or blending from time $t = 0$ to time $t = 1$ between two different poses of an elephant and a face, respectively, by computing shortest (discrete) paths. This motion is then extended (for $t < 0$ and $t > 1$) such that the resulting total path is still a shortest (discrete) path between the two new end shapes. The color encoding (second row) represents the amount of local distortion.

4 Beyond shape morphing – more than just shortest paths

So far we have discussed (discrete) shortest paths between two given shapes, which can be computed via a minimization of the (discrete) path energy. Once such a path is obtained we can also extend it beyond its initial and final shapes whilst preserving the shortest path property, as shown in Figure 6.

Furthermore, there is a natural way of transferring geometric variations from one pose of a shape to another pose. Let us assume that a (discrete) animation path has already been computed which represents for example the blending of a neutral face expression to an expression of disgust as in Figure 7 (green shapes). Additionally, we have another smiling face (top left in Figure 7) which we consider to be a *variation* of the neutral face. Now, using an extension of the techniques presented here, one can "transport" this "smiling variation" along the given (green) path leading to a different (discrete) animation path (shown in orange).

As a final result, we obtain a smiling face on top of the disgust expression (top right in Figure 7). In practice, this technique is primarily used to transport small variations. Imagine an artist wants his character to have a slightly longer nose. He realizes this variation manually only on the neutral face expression and can then use the transportation tool to apply this change to all other expressions in a consistent and automated way.

By means of the discrete path energy we are able to compute a smooth transition between *two* fixed end shapes – which can be seen as given keyframes.

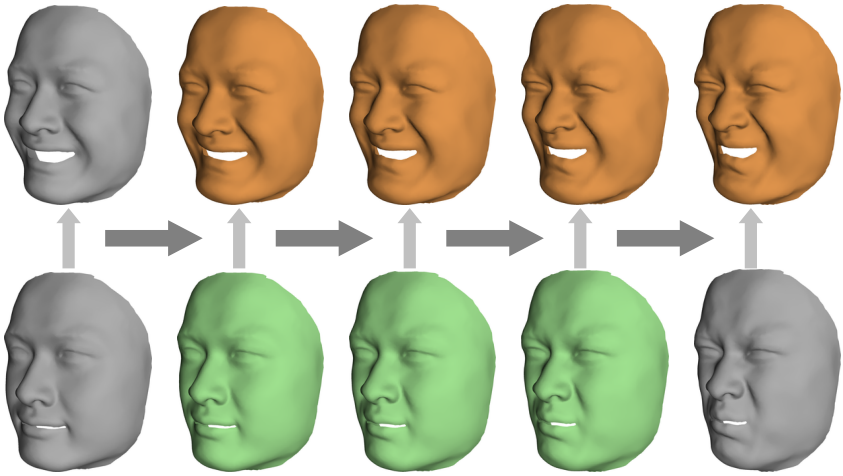

Figure 7: The face variation given by the difference between a smiling (upper left) and a neutral face (lower left) is transported along a given path (bottom row) towards a disgusted face (bottom right), resulting in a smile with a frown (upper right).

However, in applications one often has a sequence of (more than two) keyframes and aims at an *interpolation*, that is, a smooth transition path going through all of the keyframes. A straight-forward solution might be to compute a sequence of shortest discrete path between pairs of consecutive keyframes and then concatenate all segments. Although this *piecewise* approach realizes smooth transitions *between* the keyframes, it leads to visible discontinuities *at* the keyframes. A corresponding example on the sphere can be seen in Figure 8 (left), where keyframes are denoted by black dots. The solution we are looking

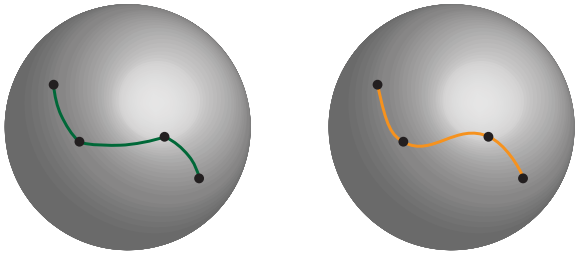

Figure 8: Piecewise (green) vs. spline (orange) interpolation on the sphere. Notice the discontinuities at the keyframes on the left.

for is shown in Figure 8 on the right and is known as *spline* interpolation. Physically, a spline of a prescribed length connecting two fixed end points is given by the connecting curve with minimal bending or curvature. In contrast, the rapid change of direction of the green curve in Figure 8 visible at the keyframes leads to high local curvature. The crucial point is that the green curve is based on a (piecewise) minimization of the path energy – which we have learned is related to minimizing the *length* of the curve.[7] To minimize the accumulated curvature along the curve, instead of the path energy, we work to minimize what is called the "spline energy". This allows the creation of smooth paths through a number of keyframes. A corresponding example in the space of geometric shapes (representing a body performing a periodic gym exercise) is shown in Figure 9.

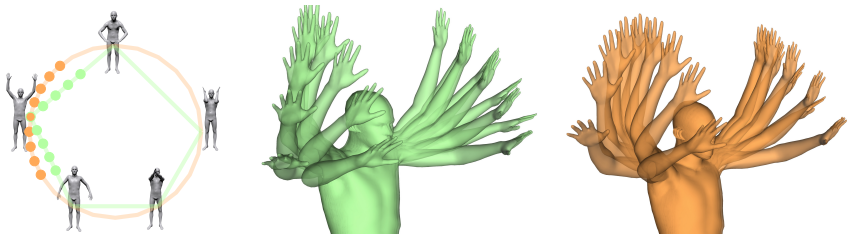

Figure 9: Piecewise (green) vs. spline (orange) interpolation in shape space. Prescribed keyframes are shown in gray (left). Notice the discontinuities at the keyframes for the green curve (middle), whereas the orange curve is globally smooth (right).

Finally, let us briefly comment on two more applications in the shape space of triangle meshes that are based on the techniques presented here. First, being able to compute shortest (discrete) paths between any two different shapes by minimizing the discrete path energy also provides a notion of a global distance, which is simply the length of that optimal path. Having the notion of a distance measure opens the door for many statistical applications. For example, the *empirical mean* $\bar{X}$ of a collection of points $X_1, \ldots, X_M$ in Euclidean space is simply defined to be

$$\bar{X} = \frac{1}{M} \sum_{i=1}^{M} X_i \,.$$

[7] The green curve in Figure 8 is actually shorter than the orange curve.

On the other hand, $\bar{X}$ can be obtained as the unique minimizer of the function

$$X \mapsto \frac{1}{2} \sum_{i=1}^{M} \mathcal{W}(X_i, X)\,,$$

with the squared Euclidean distance $\mathcal{W}(X_i, X) = \|X_i - X\|^2$. Having now a collection of geometric shapes $X_1, \ldots, X_M$, we can compute the corresponding *mean shape* $\bar{X}$ by simply replacing $\mathcal{W}$ in the formula above by our dissimilarity measure in shape space. This leads the way to more sophisticated statistical analysis; we refer the interested reader to [21, 11] for corresponding examples in shape space.

Second, the notion of *parallel transportation* (as seen in Figure 7) might be used to investigate the *curvature* of the underlying mathematical space. For example, if we transport a variation along a closed loop, the resulting transported variation will only match the original variation if the underlying mathematical space is *flat*, that is, has no curvature. Any Euclidean space is flat, whereas the sphere has a constant positive curvature. This leads to a measurable gap when transporting a variation in a loop on the sphere which (after some normalization) in turn encodes curvature information. We have used this approach, among others, to investigate the curvature of shape spaces, see [8, 4].

5 Current research and future works

In the last decade, we have investigated various applications in the shape space of triangle meshes. As outlined in this snapshot, we have always represented shapes as their vector of vertex positions since we assumed that the connectivity of the mesh does not change. Recently, we have been starting to work on two generalizations of this approach.

First, we aim at releasing the constraint of fixed connectivity. To this end, we will be able to deal with pairs of arbitrary shapes (only subject to some topological restrictions). This is an important feature for real-world applications, since faces (as shown in Figure 6), for example, often stem from sensors measuring point clouds. These point clouds are then transformed into triangle meshes. However, when transforming two measured point clouds of two different faces one obtains two different triangulations in general. As a first step in this direction, we investigated "shape matching" between two triangle meshes with different connectivities in [5].

Second, we are currently investigating different representations of geometric shapes, that is, triangle meshes are no longer represented by their vertex positions. Recall that the definition of the membrane and bending dissimilarity

measure above is based on the change of edge lengths and dihedral angles, respectively. Hence it is a promising approach to consider these quantities as primary variables – see [6, 20, 18]. To this end, all optimization happens in terms of these quantities and once we have obtained a set of optimal lengths and angles one has to reconstruct an (embedded) triangle mesh from these values. Using lengths and angles as variables has two immediate advantages: on the one hand, the dissimilarity measures become easier (note that they are quadratic in $l_e[\tilde{X}]$ and $\theta_e[\tilde{X}]$ while being highly nonlinear in $\tilde{X}$), and on the other hand this formulation is inherently invariant to global translations or rotations, which was a desired feature of our model.

Acknowledgements

Martin Rumpf and Behrend Heeren are supported by the Hausdorff Center for Mathematics at the University of Bonn, which is funded by the Deutsche Forschungsgemeinschaft (DFG, German Research Foundation) under Germany's Excellence Strategy – EXC-2047/1 – 390685813.

The authors thank Astrid Slizewski for the careful reviewing of an early version of this snapshot.

References

[1] M. Bauer, M. Bruveris, and P. W. Michor, *Why use Sobolev metrics on the space of curves*, Riemannian computing in computer vision (P. Turaga and A. Srivastava, eds.), Springer, 2016, pp. 223–255.

[2] M. Bauer, P. Harms, and P. W. Michor, *Sobolev metrics on shape space of surfaces*, Journal of Geometric Mechanics **3** (2011), no. 4, 389–438.

[3] D. Cohen-Steiner and J. M. Morvan, *Restricted Delaunay triangulations and normal cycle*, Proc. of Symposium on Computational Geometry, 2003, pp. 312–321.

[4] A. Effland, B. Heeren, M. Rumpf, and B. Wirth, *Consistent curvature approximation on Riemannian shape spaces*, 2020.

[5] D. Ezuz, B. Heeren, O. Azencot, M. Rumpf, and M. Ben-Chen, *Elastic correspondence between triangle meshes*, Computer Graphics Forum **38** (2019), no. 2.

[6] S. Fröhlich and M. Botsch, *Example-driven deformations based on discrete shells*, Computer Graphics Forum **30** (2011), no. 8, 2246–2257.

[7] P. Gladbach and H. Olbermann, *A finite-difference discretization of the Willmore functional*, (2020), in preparation.

[8] B. Heeren, M. Rumpf, P. Schröder, M. Wardetzky, and B. Wirth, *Exploring the geometry of the space of shells*, Computer Graphics Forum **33** (2014), no. 5, 247–256.

[9] ———, *Splines in the space of shells*, Computer Graphics Forum **35** (2016), no. 5, 111–120.

[10] B. Heeren, M. Rumpf, M. Wardetzky, and B. Wirth, *Time-discrete geodesics in the space of shells*, Computer Graphics Forum **31** (2012), no. 5, 1755–1764.

[11] B. Heeren, Ch. Zhang, M. Rumpf, and W. Smith, *Principal geodesic analysis in the space of discrete shells*, Computer Graphics Forum **37** (2018), no. 5.

[12] D. G. Kendall, *Shape manifolds, Procrustean metrics, and complex projective spaces*, The Bulletin of the London Mathematical Society **16** (1984), no. 2, 81–121.

[13] M. Kilian, N. J. Mitra, and H. Pottmann, *Geometric modeling in shape space*, ACM Trans. Graph. **26** (2007), no. 64, 1–8.

[14] S. Kurtek, E. Klassen, Zh. Ding, and A. Srivastava, *A novel Riemannian framework for shape analysis of 3D objects*, Proceedings of the IEEE Conference on Computer Vision and Pattern Recognition, 2010, pp. 1625–1632.

[15] A. Mennucci, A. Yezzi, and G. Sundaramoorthi, *Properties of Sobolev-type metrics in the space of curves*, Interfaces and Free Boundaries **10** (2008), no. 4, 423–445.

[16] P. W. Michor and D. Mumford, *Riemannian geometries on spaces of plane curves*, Journal of the European Mathematical Society **8** (2006), no. 1, 1–48.

[17] M. I. Miller and L. Younes, *Group actions, homeomorphisms, and matching: a general framework*, International Journal of Computer Vision **41** (2001), no. 1–2, 61–84.

[18] J. Sassen, B. Heeren, K. Hildebrandt, and M. Rumpf, *Geometric optimization using nonlinear rotation-invariant coordinates*, Computer Aided Geometric Design **77** (2020).

[19] A. Trouvé and L. Younes, *Metamorphoses through Lie group action*, Foundations of Computational Mathematics **5** (2005), no. 2, 173–198.

[20] Y. Wang, B. Liu, and Y. Tong, *Linear surface reconstruction from discrete fundamental forms on triangle meshes*, Computer Graphics Forum **31** (2012), no. 8, 2277–2287.

[21] Ch. Zhang, B. Heeren, M. Rumpf, and W. Smith, *Shell PCA: statistical shape modelling in shell space*, IEEE International Conference on Computer Vision (ICCV), 2015.

Behrend Heeren *is a postdoc in mathematics at the University of Bonn.*

Martin Rumpf *is a professor of mathematics at the University of Bonn.*

Mathematical subjects
Numerics and Scientific Computing

Connections to other fields
Computer Science

DOI
10.14760/SNAP-2020-007-EN

Snapshots of modern mathematics from Oberwolfach provide exciting insights into current mathematical research. They are written by participants in the scientific program of the Mathematisches Forschungsinstitut Oberwolfach (MFO). The snapshot project is designed to promote the understanding and appreciation of modern mathematics and mathematical research in the interested public worldwide. All snapshots are published in cooperation with the IMAGINARY platform and can be found on www.imaginary.org/snapshots and on www.mfo.de/snapshots.

ISSN 2626-1995

Junior Editors
Lara Skuppin and Sara Munday
junior-editors@mfo.de

Senior Editor
Sophia Jahns (for Carla Cederbaum)
senior-editor@mfo.de

Mathematisches Forschungsinstitut
Oberwolfach gGmbH
Schwarzwaldstr. 9–11
77709 Oberwolfach
Germany

Director
Gerhard Huisken

Mathematisches
Forschungsinstitut
Oberwolfach

Member of Leibniz Association

IMAGINARY
open mathematics